Analyst

PAPER

View Article Online
View Journal | View Issue

Cite this: *Analyst*, 2014, **139**, 5460

An electrochemical DNA biosensor for the detection of *Mycobacterium tuberculosis*, based on signal amplification of graphene and a gold nanoparticle–polyaniline nanocomposite

Chang Liu, Dongneng Jiang, Guiming Xiang, Linlin Liu, Fei Liu and Xiaoyun Pu*

Due to its low growth rate and its fastidious nature, *Mycobacterium tuberculosis* is difficult to identify. Its rapid and sensitive detection is, however, critical for the control of tuberculosis. Molecular biology, and more recently electrochemical technology, have been exploited for the detection of this pathogen. In the present study, a novel DNA biosensor was developed for the highly sensitive detection of the specific DNA insertion sequence IS6110 of *M. tuberculosis*, using reduced graphene oxide–gold nanoparticles (rGO–AuNPs) as a sensing platform and gold nanoparticles–polyaniline (Au–PANI) as a tracer label for amplification. Reduced graphene oxide, which has a large surface area, provided a biocompatible matrix. Gold nanoparticles were electrodeposited on the surface of the rGO modified electrode, which not only increased immobilisation of the capture probe but also promoted electronic transfer. The Au–PANI nanocomposite exhibited good biocompatibility and excellent electrochemical activity. It was therefore used as a tracer label for electrochemical detection, which provided a simple preparation process for a signal-on DNA biosensor. With the excellent electroactivity of the Au–PANI nanocomposite, the resulting DNA biosensor exhibited high sensitivity for the detection of *M. tuberculosis* over a broad linear range, between 1.0×10^{-15} and 1.0×10^{-9} M. The DNA biosensor showed good stability and high specificity and provides a new strategy for clinical *M. tuberculosis* diagnostics and probably also for pathogenic bacteria in general.

Received 29th May 2014
Accepted 31st July 2014

DOI: 10.1039/c4an00976b

www.rsc.org/analyst

1. Introduction

Mycobacterium tuberculosis is one of the major causes of pulmonary tuberculosis and has affected 1.7 billion people worldwide, especially in developing countries.[1] It has been estimated that the global number of tuberculosis cases is rising at a rate of 2% per year.[2] The early and accurate detection of infectious diseases represents a major challenge in humans. Rapid and sensitive detection methods for *M. tuberculosis* are thus an indispensable enhancement to laboratory diagnosis and are essential to patient management.

Conventional smear microscopy and culture methods are widely used in the diagnosis of *M. tuberculosis*. However, smear microscopy is not sensitive,[3,4] and in addition the cultures can take as long as 6–8 weeks, which limits the value of these methods in meeting the need for rapid diagnosis. Many molecular diagnostic tests, such as real-time polymerase chain reaction (PCR), DNA microarray assay and cycling probe technology, have been developed to detect *Mycobacteria* nucleic acids in sputum or culture samples.[5–7] However, most of the reliable molecular diagnostic tests are still limited by cost, time and labour requirements.

In recent years electrochemical methods have attracted considerable attention in pathogen diagnosis, due to their low cost, rapid response, sensitivity and ease of operation. Meanwhile, in biosensor design,[8,9] there has been an explosion of interest in nanomaterial synthesis and its application in the area of bioassays.[10]

Biocompatible reduced graphene oxide (rGO) possesses a unique combination of excellent exceptional thermal conductivity and a large surface area,[11,12] and it can therefore promote electron transfer and further amplify the electrochemical signal. Meanwhile gold nanoparticles (AuNPs), which combine strong adsorption ability and good conductivity, can improve both the electrical properties and the molecular stability of rGO.[13] In the present study, we constructed an electrochemical DNA biosensor with rGO–AuNPs nanocomposites as the biosensor platform. Not only does this setup increase the surface area of the electrode, it also promotes electron transfer and improves the immobilisation of the capture probe.

Polyaniline (PANI) has a polymer chain structure that provides a large specific surface area, rapid electron transfer

Department of Clinical Laboratory, Xinqiao Hospital, Third Military Medical University, Chongqing 400037, P. R. China. E-mail: xqyjyk@foxmail.com; Fax: +86-023-68755637; Tel: +86-023-68755637

dynamics and excellent electrochemical activity.[14] Moreover, due to its relatively high conductivity, thick layers can be employed for transmitting the current generated. These unique physical and chemical properties allow PANI to serve as a direct electron mediator and to further amplify the electrochemical signal. Additionally PANI, together with the biocompatible microenvironment of AuNPs, encouraged us to synthesise an Au–PANI nanocomposite. Integrating PANI with AuNPs not only improves the immobilisation of the DNA probe but also improves signal amplification. To the best of our knowledge, the development of a DNA electrochemical biosensor for *M. tuberculosis* detection based on an Au–PANI hybrid for amplification has received very little attention.

In the present study we have demonstrated a new and sensitive electrochemical DNA biosensor for the detection of *M. tuberculosis* based on the specific sequence of the IS6110 gene, and this has been validated as being both effective and sensitive.[15] In this DNA biosensor a nanocomposite of reduced graphene oxide (rGO) and AuNPs as the biosensor matrix was first assembled on a glassy carbon electrode (GCE), providing a large surface area and facilitating electron transfer for amplifying the detection response. Additionally, the Au–PANI nanocomposite was formed as the direct electron mediator. Using sandwich reactions the Au–PANI nanocomposite-labelled DNA probes were captured on an rGO–AuNPs nanohybrid-modified electrode surface. The electrochemical signal originated from the Au–PANI nanocomposite for DNA hybridisation detection. Due to the linearity of the DNA concentration and the current response, we found it possible to detect *M. tuberculosis* with good sensitivity and a low detection limit. This provides a promising mechanism that will have a broad application in a range of pathogenic microorganism analyses.

2. Experimental

2.1 Reagents and apparatus

Gold chloride ($HAuCl_4$) and hexanethiol (96%; HT) were purchased from Sigma Chemical Co. (St. Louis, MO, USA). $K_3[Fe(CN)_6]$ and poly(diallyldimethylammonium chloride) (PDDA) were purchased from Beijing Chemical Reagent Co. (Beijing, China). Graphene oxide (GO) was obtained from Nanjing Xianfeng Nano Co. (Nanjing, China). Potassium persulfate ($K_2S_2O_8$) was purchased from Shanghai Chemical Reagent Co. (Shanghai, China).

In the experimental work, 20 mM Tris–HCl buffer (pH 7.4) containing 140 mM NaCl, 5 mM KCl and 1 mM $MgCl_2$ was used as the DNA probe solution. A 0.1 M phosphate-buffered solution (PBS, pH 7.4) containing 10 mM Na_2HPO_4, 10 Mm KH_2PO_4 and 2 mM $MgCl_2$ was used as the working buffer solution. All other chemicals were of analytical reagent grade.

A DNA probe was designed for the IS6110 gene, which is *M. tuberculosis* complex-specific. All oligonucleotides were provided by Sangon Biotech. Co. Ltd. (Shanghai, China). The oligonucleotide sequences were as follows:

Target DNA: 5′-AGACCTCACCTATGTGTCGA-3′

Capture probe: 5′-GGTGAGGTCT(SH)-3′

Signal probe: 5′-SH-CCCCCCAAAAATCGACACATA-3′.

Cyclic voltammetry (CV) and differential pulse voltammograms (DPV) were conducted using a CHI660D electrochemical work station (Shanghai Chenhua Instruments, China). A conventional three-electrode configuration was used with a modified GCE (4 mm diameter) as the working electrode, a saturated calomel electrode (SCE) as reference and a platinum wire as the auxiliary electrode. The CVs of the potential range were taken between −0.2 V and 0.6 V at a scan rate of 100 mV s^{-1}. DPV measurements were performed in 0.1 M PBS (pH 7.4). The potential range was from −0.3 to +0.4 V. The scanning electron micrographs (SEM) were taken using model S-4800 (Hitachi, Japan).

2.2 Preparation of DNA samples and PCR amplification

All experiments were performed in compliance with the relevant laws and institutional guidelines, and the appropriate authorities kindly approved the experimental work.

Eight sputum samples (six positive, two negative) were collected from Xinqiao Hospital. Clinical samples were decontaminated using *N*-acetylcysteine–NaOH and subsequently concentrated by centrifugation. DNA was purified using the TaKaRa MiniBEST Bacterial Genomic DNA extraction kit (Takara Bio, Shigo, Japan), according to the manufacturer's instructions. The extracted DNA samples were retained at −20 °C for further use.

The ABI 7500 Real-Time PCR System (Applied Biosystems, Foster City, USA) was used for DNA amplification. The forward primer 5′-AGAAGGCGTACTCGA-CCTGA-3′ and the reverse primer 5′-GATCGTCTCGGCTAGT-GCAT-3′ were designed for the IS6110 sequence. For the PCR, the genomic DNA was initially denatured at 95 °C for 5 min, followed by 40 cycles at 94 °C for 30 s, 55 °C for 45 s, 72 °C for 30 s, and a final 3 min extension. The product was resolved using 2% agarose gel and visualised using a Gel Logic 212 Imaging system (Kodak, Japan).

2.3 Preparation of rGO and Au–PANI nanocomposite

Initially, according to the modified procedure,[16] rGO was prepared by adding 0.2 mL PDDA (30%) to a 50 mL stable dispersion of exfoliated graphene oxide (GO) sheets (1 mg mL^{-1}) with stirring for 30 min. Hydrazine hydrate (0.5 mL; 80%) was then added and the mixture stirred for about 12 h at 90 °C. Finally, the product was centrifuged and washed a number of times with double-distilled water.

Prior to preparing the gold nanoparticle–polyaniline nanocomposite, the AuNPs were prepared. $HAuCl_4$ solution (100 mL; 0.01%) was raised to the boil with vigorous stirring and 2.5 mL of sodium citrate solution (1%) then added immediately. The solution turned deep red, indicating the formation of colloidal gold nanoparticles, and was allowed to cool under continued stirring.

The gold nanoparticle–polyaniline nanocomposite was then prepared by adding 5 mL of 0.5 M H_2SO_4 solution to 100 mL freshly distilled aniline under continuous stirring, and 10 mL of colloidal AuNPs were then added to the aniline–H_2SO_4 solution. A 5 mL solution of $K_2S_2O_8$ (0.15 M) was added dropwise under vigorous stirring over 2 h to induce polymerisation. The Au–

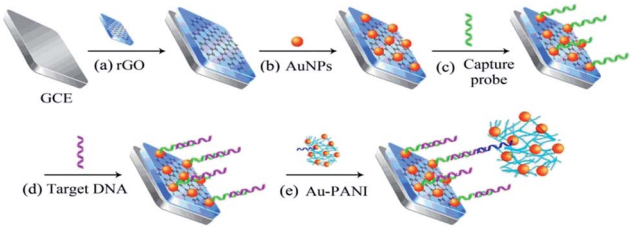

Fig. 1 Schematic illustration of the stepwise electrochemical fabrication process: (a) fabrication of rGO nanocomposite membrane; (b) formation of AuNP film; (c) immobilisation of captured DNA; (d) combination, and (e) detection of target DNA.

PANI nanocomposite obtained was centrifuged and further washed with water.

2.4 Fabrication of DNA biosensor

The rGO-coated GCE was prepared by first polishing the GCE (4 mm dia.) with 0.3 and 0.05 μm alumina powder and then washing ultrasonically separately with water and ethanol for 3 to 5 min. A total of 6 μL of rGO solution was dropped onto the pretreated electrode surface, which was then dried at room temperature. AuNPs were electrodeposited over 30 s on the rGO-modified electrode surface at a constant potential of −0.2 V. Subsequently, 20 μL of a 2.5 μM thiol-labelled capture probe solution was added to the surface of the rGO–AuNPs and incubated overnight at room temperature. A solution of hexanethiol (HT; 1 mM, 20 μL) was then placed on the modified electrode surface for 1 h to block the nonspecific binding site of the electrode. Fig. 1 shows the stepwise process for constructing the DNA sensor, and the corresponding signal amplification of Au–PANI based on DNA hybridisation assays.

2.5 Electrochemical measurements

The electrode was incubated in the required concentration of target DNA solution for 2 h at room temperature, and 5 μL of the Au–PANI labelled probe solution was dropped onto the electrode surface and incubated 2 h. Electrochemical measurements were afterwards performed using a conventional three-electrode system. DPV measurements were taken between −0.3 V and 0.4 V (*vs.* SCE) at a scan rate of 100 mV s in 0.1 M PBS (pH 7.0).

3. Results and discussion

3.1 Characterization of rGO, AuNPs and Au–PANI composite

SEM images were taken to observe the morphological features of the nanomaterials synthesised. As illustrated in Fig. 2(a), rGO showed a large lamellate and scrolled sheet, providing a large specific surface area. The UV-visible spectra of the GO and rGO are illustrated in Fig. 2(d); a GO dispersion exhibited maximum absorption at 226 nm, which is consistent with the π–π* transition of aromatic C=C bonds, while the broad absorption at 262 nm corresponded to rGO, confirming its successful preparation.

SEM was employed to further analyze the morphology of the AuNPs electrodeposited on the rGO-modified electrode surface. A large amount of significant aureatus nanoparticles was observed (Fig. 2(b)), indicating distribution of AuNPs over the surface of rGO.

When aniline was polymerised to form PANI, the abundant filiform tubules were uniform and AuNPs coverage on the PANI could be observed (Fig. 2(c)), which further confirmed the formation of the Au–PANI composite. A hybrid with porous conjugation greatly improves the effective area of the electrode surface and amplifies the electrochemical response. To further

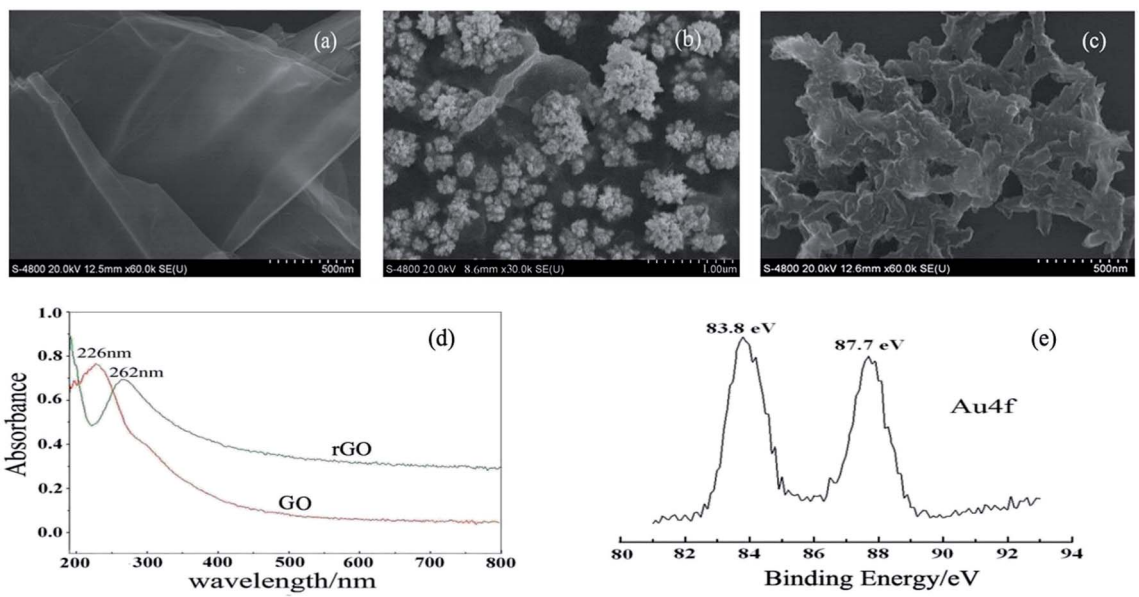

Fig. 2 Characterization of rGO, AuNPs and the Au–PANI composite: SEM images of (a) rGO, (b) AuNPs, and (c) Au–PANI nanocomposite; (d) UV-vis absorption spectra of GO and rGO suspension; (e) XPS analysis for the Au4f core-level spectrum of Au–PANI.

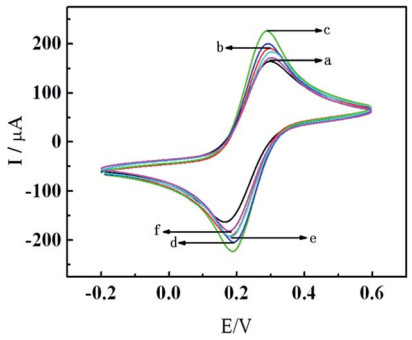

Fig. 3 Electrochemical characterization of the DNA biosensor by CVs: (a) bare GCE; (b) rGO/GCE; (c) rGO–AuNPs/GCE; (d) captured DNA/rGO–AuNPs/GCE; (e) HT/captured DNA/rGO–AuNPs/GCE; (f) combined with target DNA (1 nM).

verify the successful synthesis of Au–PANI nanocomposite, X-ray photoelectron spectroscopy (XPS) was employed. Fig. 2(e) presents the XPS signature of the Au4f doublet (83.8 eV and 87.7 eV) for the resulting metallic Au^0, which further confirmed the formation of AuNPs on PANI.

3.2 Electrochemical characterization of the DNA biosensor

The cyclic voltammetry of different modified electrodes was measured in 5 mM ferro-/ferricyanide ($Fe(CN)_6^{4-/3-}$) containing 0.1 M KCl. As shown in Fig. 3, a well-defined redox peak of Fe $(CN)_6^{4-/3-}$ occurs for the bare GCE (curve a). An increase in the peak current was observed after the modification of the rGO (curve b), which indicated that the rGO could enhance the effective surface area and the conductivity of the electrode. When the AuNPs were electrodeposited onto the rGO-modified electrode, the peak current was further increased due to the AuNPs, which facilitated electron transmission (curve c). After the thiolated capture probe was self-assembled onto the rGO–AuNPs-modified electrode surface, the peak current decreased, which suggested that the DNA blocked the electron transfer (curve d). A further decrease in peak current was observed after the electrode was treated with HT, due to its non-electroactive properties obstructing electron transfer (curve e). The redox peaks decreased again when the target DNA solution was dropped onto the electrode surface for 2 h, indicating that the oligonucleotides of the target DNA were successfully hybridised with the capture probe (curve f).

To demonstrate that the rGO–AuNPs could improve the surface area of the DNA biosensor, CVs in 5.0 mM Fe $(CN)_6^{4-/3-}$ solution containing 0.1 M KCl at different scan rates (ν) were studied. The electroactive surface area (A) of the ordinary ECG bare electrode and the rGO–AuNPs-modified electrode were determined using the Randles–Sevcik equation (1):

$$i_p = 2.69 \times 10^5 A \times D^{1/2} n^{2/3} C \nu^{1/2}, \quad (1)$$

in which i_p = maximum current (amps), n = number of electrons transferred, D = diffusion coefficient ($cm^2\ s^{-1}$), A = electrode area (cm^2), C = concentration (mol cm^{-3}) and ν = scan rate (s). As shown in Fig. 4(a) and (b), by using the constant parameters D, C and n we were able to calculate the electroactive surface area (A) of the ECG bare electrode as 11.2 mm^2 and that of the rGO–AuNPs modified electrode as 19.35 mm^2. Compared with the ECG bare electrode, the electroactive surface area of the rGO–AuNPs-modified electrode was increased by approximately 72.7%.

3.3 Analytical performance of the DNA biosensor

The DPV responses for synthetic target oligonucleotides at different concentrations were recorded in 1 mL of 0.1 M PBS (pH 7.0). From Fig. 5(a), we can observe that the reduction peak current increases with increasing concentration of the target DNA solutions. The calibration curves in Fig. 5(b) show a linear relationship from 1 fM to 1 nM between the reduction peak current and the concentration of the target DNA. Compared with other previously reported methods for the detection of *M. tuberculosis*, it is clear that the electrochemical DNA biosensor based on the rGO–AuNPs-modified electrode and the Au–PANI-assisted signal amplification strategy had significantly improved the sensitivity and linear range of the proposed DNA sensor.

3.4 Selectivity and stability of the DNA biosensor

To investigate the specificity of the biosensor designed, the PCR products of four respiratory-related bacterial samples (*Staphylococcus aureus*, *Mycoplasma pneumoniae*, α-haemolytic *Streptococcus*, and *Streptococcus pneumoniae*), and a mixture of these

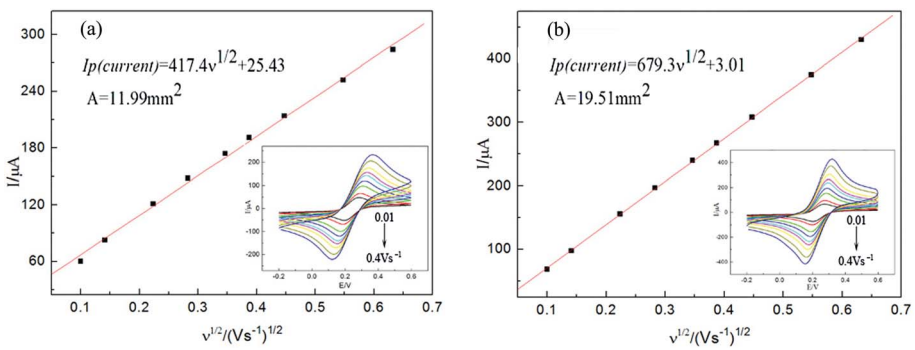

Fig. 4 Electroactive surface area of the electrode by CVs: (a) bare GCE, and (b) rGO–AuNPs-modified GCE in 5.0 mM Fe $(CN)_6^{4-/3-}$ at different scan rates.

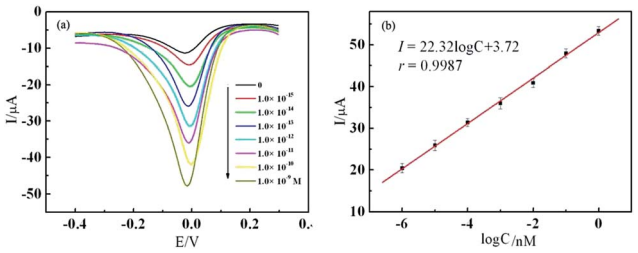

Fig. 5 Analytical performance of the DNA biosensor: (a) DPVs of the electrochemical biosensor for target DNA detection at concentrations between 0 and 1.0×10^{-15} M, and (b) the calibration plot of DPV peak current *vs.* log *C* nM ranges between 1.0×10^{-15} and 1.0×10^{-9} M.

samples, were assessed. As illustrated in Fig. 6(a) and (b), the DPV responses to the PCR products of the four interferences were close to that of the blank sample. However, there was a significant electrochemical signal from the target DNA, even though the other four interferences were mixed with the target DNA solution. The results illustrated that the biosensor had excellent specificity for the detection of *M. tuberculosis*.

In the present study, the stability of the DNA biosensor was investigated. As observed in Fig. 6(c), the stability of successive assays was studied over 50 cycles of CV measurements in PBS after incubation with 100 pM of *M. tuberculosis*. The result suggests that the peak current had decreased by only 3.7%. Additionally, we demonstrated the stability of the biosensor using a long-term storage assay. After 20 days' storage at 4 °C, the electrochemical signal retained 91.7% of its initial value, indicating that the stability was sufficient for use in the detection of *M. tuberculosis*.

3.5 Analysis of clinical samples, and comparison with PCR

The practicability of applying the proposed electrochemical biosensor clinically was assessed by analysing eight clinical sputum samples (S1–S5 positive and S6–S8 negative), which had initially been detected by PCR amplification. The PCR products were identified by running 10 μL of a PCR mixture in 2% agarose gel for 30 min and observing the samples under ultraviolet light. In the case of samples S1 to S5, agarose gel electrophoresis revealed products of the correct size (157 bp), whereas samples S6 to S8 were negative (Fig. 7(a)). The proposed electrochemical DNA biosensor was then applied to the PCR samples. The peak current of DPV correlated with the PCR bands from the positive samples, S1 to S5. Meanwhile, there was hardly any DPV response from samples S6 to S8, which was again consistent with the PCR detection results (Fig. 7(b) and (c)).

PCR analysis requires standardisation for sampling, a complicated reaction protocol and strict laboratory conditions.

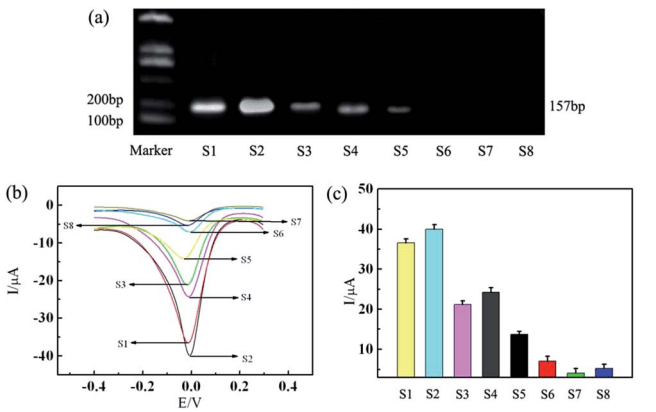

Fig. 7 A comparative analysis with PCR: (a) gel electrophoresis photographs of PCR products obtained from S1 to S8; (b) DPV curves for the detection of S1 to S8; and (c) DPV peak currents responding to the PCR products obtained from S1 to S8.

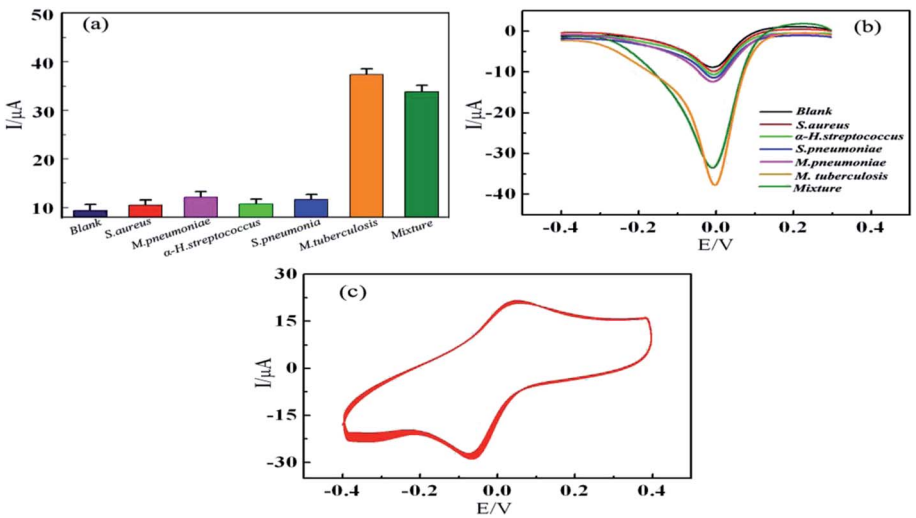

Fig. 6 Selectivity and stability of the DNA biosensor: (a) selectivity of the DNA biosensor, using four different PCR products (1 nM) as interferences, and a mixture of the above four interferences and *M. tuberculosis* (1 nM); (b) DPV curves for detection of the four different PCR products, *M. tuberculosis* and the mixture; and (c) stability of the DNA biosensor under successive CV scans for 50 cycles after incubating with 100 pM target DNA.

The PCR method has distinct advantages in sensitivity, but false positives often occur, and the low resolution of post-PCR analysis by gel electrophoresis also limits its routine use by a number of laboratories. In contrast, the detection process of the proposed biosensor is simple and easy to operate and may be used in point-of-care testing. Moreover, the proposed strategy has exhibited high specificity and sensitivity, which demonstrates its potential as a pragmatic tool for *M. tuberculosis* testing in clinical samples.

4. Conclusions

Since the identification of *M. tuberculosis* by Robert Koch in 1882, TB diagnosis has always remained a challenge. There have been a large number of reports concerning diagnostic techniques for detecting *M. tuberculosis*.[17,18] In addition to improved sensitivity and specificity, however, an innovative strategy for diagnosis must also embody simplicity, rapidity and the capability of becoming a point-of-care test.

The present study has demonstrated a highly sensitive electrochemical DNA detection platform based on a signal amplification strategy, using a reduced graphene oxide–gold nanoparticle-modified electrode and a probe-labelled Au–PANI nanocomposite as amplification. The rGO–AuNPs dramatically enlarge the surface area and enhance electronic transfer. In addition, the outstanding electrical conductivity of Au–PANI can increase the sensitivity for the detection of *M. tuberculosis* DNA down to the fm level. Moreover, the proposed method demonstrates excellent ability for assessing clinical samples based on highly specific DNA probes for the IS6110 gene sequence, This novel technique provides a simple, versatile and powerful tool for reliable diagnosis, and the technique is suitable not only for detecting *M. tuberculosis* but could equally be applied to other bacteria.

Acknowledgements

The authors are grateful to the National Natural Science Foundation of China (NSFC 81371898) for financial support. We also appreciate the constructive comments received from all the members of our laboratories.

References

1 M. Arentz and T. R. Hawn, *Drug Discovery Today: Dis. Mech.*, 2007, **4**, 231–236.
2 P. C. Soo, Y. T. Horng, K. C. Chang, J. Y. Wang, P. R. Hsueh, C. Y. Chuang, C. C. Lu and H. C. Lai, *Mol. Cell. Probes*, 2009, **23**, 240–246.
3 M. Caws, S. M. Wilson, C. Clough and F. Drobniewski, *J. Clin. Microbiol.*, 2000, **38**, 3150–3155.
4 K. R. Steingart, V. Ng, M. Henry, P. C. Hopewell, A. Ramsay, J. Cunningham, R. Urbanczik, M. D. Perkins, M. A. Aziz and M. Pai, *Lancet Infect. Dis.*, 2006, **6**, 664–674.
5 R. Sanjuan-Jimenez, P. Morata, P. Bermudez, M. J. Bravo and J. D. Colmenero, *PLoS Neglected Trop. Dis.*, 2013, **7**, e2593.
6 M. Fukushima, K. Kakinuma, H. Hayashi, H. Nagai, K. Ito and R. Kawaguchi, *J. Clin. Microbiol.*, 2003, **41**, 2605–2615.
7 R. Pahwa, S. Hedau, S. Jain, N. Jain, V. M. Arora, N. Kumar and B. C. Das, *J. Med. Microbiol.*, 2005, **54**, 873–878.
8 Y. Du, C. G. Chen, M. Zhou, S. J. Dong and E. K. Wang, *Anal. Chem.*, 2011, **83**, 1523–1529.
9 S. J. Guo and E. K. Wang, *Anal. Chim. Acta*, 2007, **598**, 181–192.
10 L. Wang, C. Z. Zhu, L. Han, L. H. Jin, M. Zhou and S. J. Dong, *Chem. Commun.*, 2011, **47**, 7794–7796.
11 L. Jiang, R. Yuan, Y. Chai, Y. Yuan, L. Bai and Y. Wang, *Analyst*, 2012, **137**, 2415–2420.
12 S. Park and R. S. Ruoff, *Nat. Nanotechnol.*, 2009, **4**, 217–224.
13 S. Stankovich, D. A. Dikin, G. H. B. Dommett, K. M. Kohlhaas, E. J. Zimney, E. A. Stach, R. D. Piner, S. T. Nguyen and R. S. Ruoff, *Nature*, 2006, **442**, 282–286.
14 C. Dhand, M. Das, M. Datta and B. D. Malhotra, *Biosens. Bioelectron.*, 2011, **26**, 2811–2821.
15 S. H. Montenegro, R. H. Gilman, P. Sheen, R. Cama, L. Caviedes, T. Hopper, R. Chambers and R. A. Oberhelman, *Clin. Infect. Dis.*, 2003, **36**, 16–23.
16 L. L. Li, K. P. Liu, G. H. Yang, C. M. Wang, J. R. Zhang and J. J. Zhu, *Adv. Funct. Mater.*, 2011, **21**, 869–878.
17 H. H. Wang, C. Y. Zhao and F. Li, *Braz. J. Microbiol.*, 2011, **42**, 964–972.
18 M. Gazouli, E. Liandris, M. Andreadou, L. A. Sechi, S. Masala, D. Paccagnini and J. Ikonomopoulos, *J. Clin. Microbiol.*, 2010, **48**, 2830–2835.